International Journal of Current Engineering and Technology
E-ISSN 2277 – 4106, P-ISSN 2347 – 5161
©2016 INPRESSCO®, All Rights Reserved
Available at http://inpressco.com/category/ijcet

Research Article

Defluoridation of Drinking Water by Glucamine-Modified Ordered Mesoporous Silica Type SBA-15

Taissire Ben Amor†* , Anissa Hamrouni, Mohamed Tlili and Mohamed Ben Amor

†Laboratoire de Traitement des Eaux Naturelles. Centre de Recherches et Technologies des Eaux (CERTE), Technopole de Borj-Cédria, 8020 Soliman, Tunisia.

Accepted 08 Sept 2016, Available online 31 Oct 2016, **Vol.6, No.5 (Oct 2016)**

Abstract

The present survey highlights for the first time that glucamine-modified ordered mesoporous silica (OMS) type SBA-15 can be used as adsorbents for the uptake of fluoride from water. By means of X-Ray Diffraction, N_2 adsorption-desorption, Thermogravimetry and Fourier transform InfraRed the structure and physicochemical properties of the materials were characterized. The behavior of the calcined and glucamine modified SBA-15 in adsorption of fluoride from solutions were investigated. Batchwise adsorption test of prepared adsorbent was carried out in aqueous sodium fluoride solution and natural water containing fluoride ions. Physico-chemical parameters such as adsorbent dose, equilibrium contact time, pH, initial fluoride concentration and co-existing anions were studied in a series of batch adsorption experiments. fluoride adsorption on the adsorbent was saturated within 3 hours in solution containing 2 mg L^{-1} of fluoride, with 2 g L^{-1} of adsorbent dose. The maximum adsorption of fluoride on the adsorbent could be obtained in the solution at about pH 3. The pH changes during the adsorption process suggested that the OH on the surface of OMS type SBA-15 was the adsorption sites. Comparative studies for fluoride removal in synthetic as well as natural water showed relatively higher fluoride removal in synthetic water.

Keywords: *Defluoridation, OMS SBA-15, Grafting, adsorption.*

1. Introduction

In many region of the world, drinking water suffers from presence of natural contaminant such as fluoride, nitrate, sulfate, which cause large-scale health problems. Fluoride is an essential component for normal mineralization of bones and formation of dental enamel (Bell and Ludwing, 1970). However, excessive intake could result in teeth mottling, dental and skeletal fluorosis (Susheela, *et al*, 1993). The safe limit of fluoride in drinking water is different from one country to another depending on climatic conditions (Meenakshi and Maheshwari, 2006). Indeed, as the amount of water consumed and consequently the amount of fluoride ingested is influenced primarily by air temperature (Meenakshi and Maheshwari, 2006). The US Public Health Service has set a range of concentrations for maximum allowable fluoride in drinking water (USPHS, 1962).

Many technologies have been applied to remove fluoride from water: chemical precipitation (Islam and Patel, 2007), membrane technology (Arora, *et al*, 2004), floculation and electrocoagulation (Hu, *et al*, 2005), ion exchange (Meenakshi and Viswanathan, 2007), adsorption (Ku and Chiou, 2002) [Among various methodologies, adsorption process is the most promising for removal of fluoride from water. This offers satisfactory results especially with mineral-based and/or surface modified adsorbents.

Many adsorbents have been proposed for defluoridation which includes mineral clays (Srimurali, *et al*, 1998)metal oxide materials (Kamble, *et al*, 2007- Wajima, *et al*, 2009), activated alumina (Maliyekkal and Sharma,2006), synthetic hydroxyapatite (Gao, *et al*, 2009), zeolites (Gómez-Hortigüela, *et al*, 2013), ordered mesoporous materials (Xu, *et al*, 2001), natural calcium-rich promising adsorbents such as cuttlefish (Ben Nasr, *et al,* 2011), shell carbon of fruit and nuts (Sivasankara, *et al*, 2012- Ramírez-Montoyaa, *et al*, 2014).

In the last few decades, a very few studies have been conducted using Ordered Mesoporous Silica (OMS) for the purpose of fluoride removal. OMS are materials of choice to introduce organic functional groups, through their regular porosity, pore size, high surface area and large pore volume. Moreover, the amorphous nature of the structure offers a large number of silanols (Si-OH) that can react with different species. One of the members of this materials type, named SBA-15, discovered in 1998 by Zhao *et al*. (Zhao, *et al*, 1998) is a two-dimensional, hexagonally ordered pore structure. OMS type SBA-15 exhibits a

*Corresponding author: **Taissire Ben Amor**

large pore diameter (from 50 to 150 Å) and thick pore wall which gives to the material a higher hydrothermal stability compared to the other OMS families.

To our knowledge, OMS type SBA-15 has not been previously used as an adsorbent for fluoride removal. The only study reported in the literature present the fluoride removal utilizing a nano-composites Hydroxyapatite/Al-MCM-41 or Al-SBA-15 (Anunziata, *et al*, 2009). The authors have shown that the incorporation of Al-SBA-15 (which is a non-pure silicic OMS) within the hydroxyapatite, improves the fluoride adsorption of the nano-composite.

In the present work, our goal was to develop a novel sorbent material allowing the increase of fluoride removal capacity. For this purpose, silicic OMS type SBA-15 was functionalized with N-methyl-D-glucamine and tested for its efficiency on fluoride adsorption from fluorinated solutions with less than 5 mg/L concentrations of fluoride to make it drinkable.

2. Experimental

2.1 Synthesis of SBA-15

A typical procedure suggested by Zhao *et al*. (Zhao, *et al*, 1998) was followed Pluronic P123 ($[(EO)_{20}(PO)_{70}(EO)_{20}]$, Aldrich, 3.5 g) was dissolved in HCl (37 wt.%, Riedel de Haën, 12 m,16.5 mL) and H_2O (111.75 mL). The mixture was heated at 40 °C and maintained at this temperature under vigorous stirring for 3 h. After complete dissolution of the surfactant, tetraethylorthosilicate (TEOS, Aldrich, 7.426 g) was rapidly added to the initial solution. For the ripening step, the mixture was stirred for 24 h at the same temperature as that used for the P123 dissolution step. The starting molar ratio was TEOS/P123/HCl/H_2O = 1.0:0.017:5.6:174. After ripening, the mixture was transferred into an oven for further condensation at 90 °C under static conditions for 24 h. Finally, the products were recovered by filtration, washed with distilled water (2x100mL), and dried at 70 °C for 48 h. To eliminate the template and liberate the porosity, the as-synthesized samples were subjected to calcination in muffle furnace (NAGAT furnace, with a Gulton West 2050 temperature regulator) which was performed at 500 °C in air for 4 h with a heating rate of 1.33 °C/min.

2.2 Post-Synthesis Grafting of SBA-15 with N-methyl-D-glucamine

Calcined SBA-15 materials were functionalized by post-synthesis grafting of glucamine groups. Grafting was performed in two steps. Before grafting, calcined SBA-15 (750 mg) was heated under vacuum at 100 °C for 12 h to remove physisorbed water. The air-dried calcined SBA-15 materials were then placed in a Schlenk flask with 15 ml of anhydrous chloroform and 1.5 ml of (3-bromopropyl) trimethoxysilane (BPTMS). After evacuation and subsequent argon back-filling, the mixture was gently stirred at 65 °C under reflux for 7 h. The product was collected by Buchner filtration washed by dispersing the material in a mixture of (1:1) diethylether and dichloromethane, then left under stirring overnight at room temperature. The material is then filtered, dried in an oven at 70 °C. The grafted material was subsequently introduced in a Schlenk flask with 50 ml of an aqueous N-methyl-D-glucamine (NMDG) solution of 8 g L^{-1}, kept under reflux at 70 °C and stirred for 7 h. The glucamine grafted SBA-15 was then filtered and washed by dispersing the material in 100 ml of distilled water stirred overnight at room temperature, then filtered and dried at 70 °C overnight. Grafting reaction was reproduced several times and all samples exhibit similar characteristics.

2.3 Characterization of Materials

The calcined and grafted samples were characterized by X-ray Diffraction (XRD) with Cu anode ($\lambda_{K\alpha}$= 0.15418 nm, $0.5<2\theta<10°$, 0.02/s) at room temperature with an X'Pert PRO diffractometer (PANalytical). Nitrogen adsorption/desorption isotherms were performed with an ASAP 2420 (Micromeritics) at –196 °C. Prior to the measurements, the calcined samples were outgassed at 50 °C for 1 h then at 100 °C overnight under 1.33 Pa. The specific surface area S_{BET} was calculated by using the Brunauer–Emmett–Teller (BET) method in the range of relative pressure (p/p°) from 0.03 to 0.2 (Brunauer, *et al*, 1938). The average pore diameters were evaluated by the Broekhoff–de Boer (BdB) method applied to the desorption branch (Broekhoff and de Boer, 1968).

Thermogravimetric analyses were performed with a SENSYS evo TG-DSC (SETARAM) apparatus. Approximately 12 mg of sample were heated in flowing air (20 mL/min of N_2 and 5 mL/min of O_2) from 25 to 750 °C at a heating rate of 5 °C/min.

2.4 Fluoride adsorption experiments

For the fluoride adsorption thermodynamics, 0.1 g of the adsorbent was equilibrated with 50 mL of aqueous solution at the desired initial fluoride concentration, contact time and pH. All the adsorption experiments were carried out using a magnetic Multistirrer VELP scientifica with a stirring speed of 300 rpm. The solution pH was adjusted with dilute HCl solutions. The adsorption was carried at room temperature. Fluoride concentration before and after adsorbent treatment were measured by the fluoride specific ion electrode technique.

3. Results and discussion

3.1 Characterization of as-synthesized and grafted SBA-15 materials

The parent and grafted materials have been analyzed by XRD (Fig. 1). The two samples exhibit 3 peaks corresponding to (100), (110) and (200) reflections characteristic of a 2-D hexagonal structure as expected for SBA-15 materials.

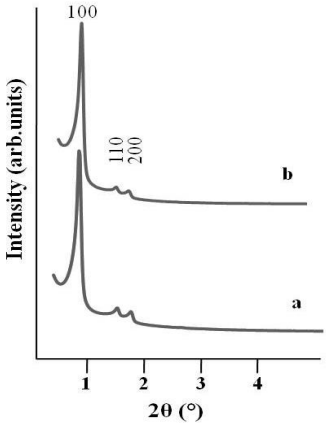

Fig.1 Small Angle X-ray diffraction patterns of calcined (a) and post-synthesis grafted (b) samples

Unit cell parameters a_{hex} are reported for each sample in Table 1. After grafting the unit cell parameter remains the same.

Table 1 Structural and textural properties of calcined and post-synthesis grafted samples

Samples	S_{BET}[a] (m^2/g)	C_{BET}[b]	D_{BdB}[c] (Å)	D_{BJH}[d] (Å)	V_p[e] (cm^3/g)	V_{mes}[f] (cm^3/g)	V_{mic}[g] (cm^3/g)	t[h] (Å)	a[i] (Å)
SBA-15 c	1000	201	78	62	1.00	0.72	0.28	32	107
SBA-15 c g	300	78	68	60	0.41	0.31	0.10	43	108

[a] BET specific surface area, [b] C_{BET} Parameter, [c] mesopore diameter calculated from the desorption branch by BdB method, [d] maximal pore diameter determined by BJH method from the desorption branch, [e] total pore volume deduced from nitrogen adsorbed volumes measured at the beginning of the plateau after the capillary condensation step, [f] mesopore volume, [g] micropore volume, [i] wall thickness ($t=a_c - 0.95\ D_{BdB}$), [j] unit cell parameter of calcined and grafted samples

Type IV nitrogen adsorption/desorption isotherms with a hysteresis loop of H1 type were obtained for the samples (Fig. 2). The branches of adsorption/desorption are parallel and vertical for the calcined SBA-15 (S-c) , however the glucamine modified SBA-15 (S-c g) sample exhibits adsorption/desorption branches parallel but with a weaker slope than the other sample. This change is probably due to a disruption of the silica matrix caused by the presence of an HBr excess in the reaction mixture due to the hydrolysis of the bromosilane moieties of the first step grafting agent. Furthermore, the isotherm of the grafted sample shows a very slight second step on the desorption branch resulting from a partial mesopores blocking following grafting.

A decrease of the nitrogen adsorbed volume in the relative pressure range between $0.2 \leq p/p° \leq 0.6$ and a slight shift of the hysteresis to the low relative pressure (p/p°) values was observed indicating a decrease of both the specific surface area and the pore size of the grafted sample compared to the parent material. The structural and textural characteristics of the starting material together with the grafted ones are reported in Table 1.

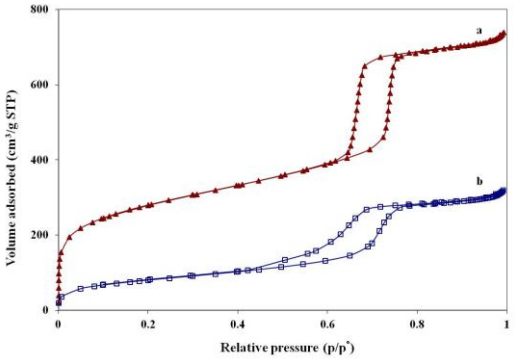

Fig.2 Nitrogen adsorption/desorption isotherms of calcined (a) and post-synthesis grafted (b) samples

The specific surface area (S_{BET}), the pore diameter (D) determined by the BdB or BJH methods from the desorption branch, the total pore volume (V_p), the meso- and micropore volume (V_{mes} and V_{mic}) of the grafted samples are lower than those of the parent SBA-15 material. These decreases are due to the occupation of the inner and outer surface of SBA-15 type OMS by the grafted groups. Similarly, the C_{BET} value of the functionalized sample is lower than the ungrafted one. Indeed, the C_{BET} parameter is a constant measuring the adsorption force of the first nitrogen adsorption layer. Thus C_{BET} is directly related to the affinity of nitrogen to the material surface (Brunel, *et al*, 2000- Jelinek and E. Kovhts, 1994). The decrease of the C_{BET} value is induced by the low affinity of nitrogen with the surface due to the presence of organic functionalities indicating a more hydrophobic surface. It is also noteworthy that the wall thickness (t) increases after grafting. In addition, the ratio V_{mes}/V_{mic} of the samples, before and after grafting, are relatively close indicating that the grafting has occurred in both micropores and mesopores of the parent material.

Thermogravimetric analyzes were performed to determine the physisorbed water loss of the materials after grafting which corresponds to the weight loss recorded between room temperature and 150 °C (Table 2).

Table 2 Physisorbed water, dehydroxylation and/or grafted organic groups weight losses (%) determined by TGA in the temperature range between 20 and 750 °C

Samples	Physisorbed water loss %	Dehydroxylation and/or graft loss %
SBA-15 c	14.4	3.6
SBA-15 c g	2.4	25

Furthermore, the weight loss detected between 150 and 750 °C corresponds to dehydroxylation and /or decomposition of the grafted groups. As those two phenomena are overlapping, only the sum of these weight losses is reported in Table 2.

After grafting, the amount of physisorbed water decreases significantly from 14.4% for the parent material to 2.4%. These results give an idea of the

hydrophobic character of the material. The weight loss observed for temperature above 150 °C increases after grafting from 3.6% attributed only to the dehydroxylation to 25% attributed to dehydroxylation and decomposition of organic agent.

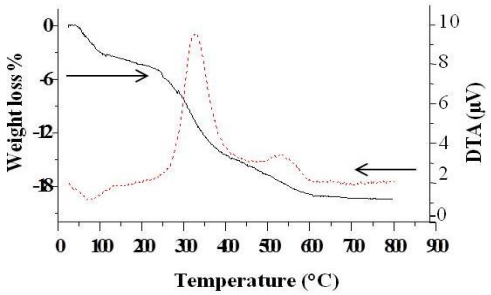

Fig.3 TGA and DTA curves of the post-synthesis grafted sample

The two exothermic bands observed at 340 and 550°C on the DTA curve (Fig.3) of the grafted SBA-15 sample are characteristic of NMDG decomposition (Reinert, *et al*, 2011).

Functional groups identified by FT-IR spectra (Fig.4) confirm that the grafting of glucamine agent on SBA-15 materials took place.

Two new bands were observed after grafting at 686 and 2958 cm^{-1} attributed to the bending and stretching vibration of C-H bond, respectively. Those bands characteristic of the organic molecules confirmed the efficiency of the grafting.

Also, a decrease of the band at 962 cm^{-1} attributed to the stretching vibration of SiO-H suggesting the reduction of silanols on the surface of silica (Bois, *et al*, 2003).

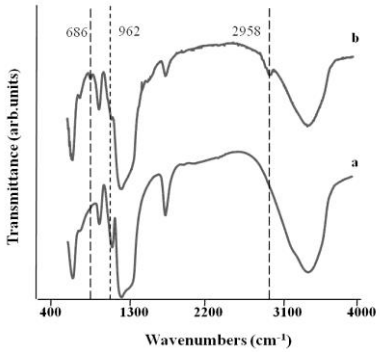

Fig. 4 FTIR spectra of the of calcined (a) and post-synthesis grafted (b) samples

3.2. Adsorption experiments

The optimization of fluoride adsorption conditions was performed on the parent material. For a constant amount of adsorbent, 100 mg of SBA-15 c, was suspended in the synthetic fluoride sodium aqueous solution $[F^-]$=2 $mg.L^{-1}$ and the contact time was varied from 3 to 24 h. The concentration of fluoride ions is constant in time. The retention of fluoride is not significant, the contact time remains fixed at three hours.

The amount of adsorbent was then varied from 100 to 400 mg for a constant contact time of 3h with $[F^-]$= 2 mg L^{-1}. The fluoride adsorption capacity increases slightly by increasing the adsorbent dose.

The concentration of fluoride was also varied between 2 and 5 $mg.L^{-1}$, for 100 mg of adsorbent and a contact time of 3h. Likewise, a very negligible change after the concentration increase.

The pH of the medium is a very important variable. We conducted a series of tests with three pH values. From the graph presented in figure 5 the lower the pH of the solution the higher the adsorption rate of fluoride. The highest fluoride rate removal (18%) obtained at pH equal to 3.

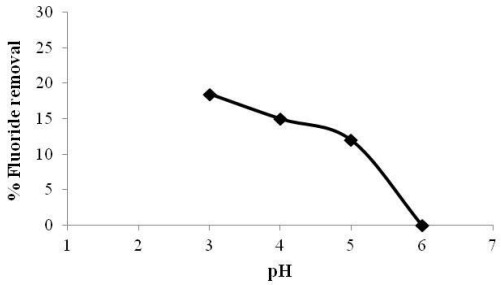

Fig. 5 Percentage of fluoride ions adsorbed as a function of solution pH

After having set the optimum adsorption conditions using the unmodified SBA-15 as adsorbent. Those conditions were applied using glucamine grafted SBA-15 (SBA-15 C g) as adsorbent.

The glucamine modified SBA-15 presented a higher adsorption capacity compared to the unmodified SBA-15 sample. The adsorption capacity was doubled after grafting (50% fluoride removal).

Table 3 Comparaison of fluoride adsorption of the unmodified and grafted SBA-15 for synthetic and natural water

	Synthetic water	Natural water
Adsorbents	% Fluoride removal	
SBA-15 C	18	20
SBA-15 C g	50	35

In the following section we will present the adsorption tests performed on a natural water rich on fluoride ions. Likewise, the grafted SBA-15 exhibit a higher rate of fluoride uptake compared to the unmodified one. However, the adsorption rate of the two tested materials is lower than that realized on fluorinated synthetic water. The fluoride adsorption rates of the unmodified and grafted SBA-15 are reported in Table 3.

The fluoride removal efficiency in natural water was found to be slightly decreased as compared to synthetic water as shown in Table 3. This may be due

to the presence of various competing ions in natural water.

3.2.1. Effect of co-existing ions on fluoride uptake

The effects of co-existing ions, including SO_4^{2-}, HCO_3^-, Cl^- and NO_3^-, usually present in natural water samples, have been investigated in the batch adsorption study. The initial concentration of natural water equal to 2 mg L^{-1} was maintained at pH 3. The results indicated that fluoride adsorption was drastically reduced to 35% on the increase in SO_4^{2-} ion concentration (Fig.6).

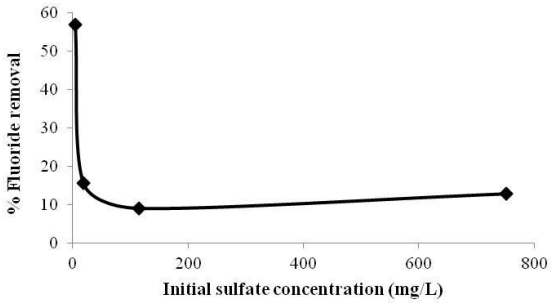

Fig.6 Effect of initial sulfate concentration on fluoride removal

The increase in the concentrations of other anions has relatively no effect on the fluoride uptake. The reduction in the fluoride removal in the presence of the sulfate ion may be attributed to the facts that the sulfate ion may have competition with the fluoride ion for the same sorption sites. The presence of the sulfate ion, being divalent, may have increased the columbic repulsive forces leading to the reduced probability of fluoride interaction with the active sites. It is also reported that the multi-charge anions get adsorbed more easily than the monovalent anions (Liang, 2007).

Conclusion

The functionalization of SBA-15 with N-methyl-D-glucamine has been described and shown to be an efficient route for fluoride removal. After synthesis, grafting and characterization, fluoride uptake efficiency was investigated and it was found that 100 mg of adsorbent dose in 2 mg L^{-1} fluoride solution and a contact time of 3h are the optimum conditions. Efficient adsorption took place at pH=3. The glucamine-modified SBA-15 presents a fluoride adsorption capacity higher than the unmodified SBA-15. However, the adsorption efficiency decreases in the presence of sulfate ions.

References

M. C. Bell (1970), The supply of fluoride to man: ingestion from water, in: Fluorides and Human Health, WHO Monograph Series 59, World Health Organization, Geneva.

A.K. Susheela (1993), A. Kumar, M. Bhatnagar, Prevalence of endemic fluorosis with gastro-intestinal manifestations in people living in some north-indian villages, *Fluoride,* 26, pp. 97-104.

S. Meenakshi and R.C. Maheshwari (2006), Fluoride in drinking water and its removal, *J. Hazard. Mater. B*. 137, pp. 456-463.

US Public Health Service (1962) Drinking Water Standards, US Government Printing Office, Department of Health Education and Welfare, Washington, DC.

M. Islam and R. K. Patel, (2007), Evaluation of removal efficiency of fluoride from aqueous solution using quick lime, *J. Hazard. Mater.* 143, pp. 303-310.

M. Arora (2004), Use of membrane technology for potable water production, *Desalination*, 170, pp. 105-112.

C.Y. Hu, (2005), Effects of the molar ratio of hydroxide and fluoride to Al(III) on fluoride removal by coagulation and electrocoagulation, *J. Colloid. Interface. Sci.* 283, pp. 472-476.

S. Meenakshi and N. Viswanathan, (2007) Identification of selective ion-exchange resin for fluoride sorption, *J. Colloid. Interface. Sci.* 308,pp. 438-350.

Y. Ku and H. M. Chiou, (2002) The adsorption of fluoride ion from aqueous solution by activated alumina, *Water Air Soil Pollut.* 133,pp. 349-360.

A. Srimurali, (1998), A study on removal of fluorides from drinking water by adsorption onto low-cost materials, *Environmental Pollution*, 99, pp. 285-289.

S. Kamble, (2007*), Defluoridation of drinking water using chitin, chitosan and lanthanum-modified chitosan, Chem. Engin . J*, 129**,**pp. 173–180.

T. Wajima, (2009), *Adsorption behavior of fluoride ions using a titanium hydroxide-derived adsorbent*, *Desalination*, 249, pp. 323–330.

S. M. Maliyekkal (2006) Manganese-oxide-coated alumina: A promising sorbent for defluoridation of water, *water research*, 40, pp. 3497 – 3506.

S. Gao, (2009) Size-dependent defluoridation properties of synthetic hydroxyapatite, *Journal of Fluorine Chemistry*, 130,pp. 550–556.

L. Gómez-Hortigüela, (2013) Natural zeolites from Ethiopia for elimination of fluoride from drinking Water*, Separation and Purification Technology*, 120, pp. 224–229.

Y-M. Xu, (2001) Preparation and Defluorination Performance of Activated Cerium(IV) Oxide/SiMCM-41 Adsorbent in Water, *Journal of Colloid and Interface Science*, 235, pp. 66–69.

A. Ben Nasr (2011) Removal of fluoride ions using cuttlefish bones, *Journal of Fluorine Chemistry*, 132,pp. 57–62.

V. Sivasankara, (2012) *Tamarind (Tamarindus indica) fruit shell carbon: A calcium-rich promising adsorbent for fluoride removal from groundwater, Journal of Hazardous Materials*, ,225– 226, pp. 164– 172

L.A. Ramírez-Montoyaa, (2014) *Preparation, characterization and analyses of carbons with naturaland induced calcium compounds for the adsorption of fluoride*, Journal of Analytical and Applied Pyrolysis, , 105, pp. 75–82.

D. Zhao, (1998) Triblock copolymer synthesis of mesoporous silica with periodic 50 to 300 angstrom pores, *Science*. 279 pp. 548-552.

O. A. Anunziata, (2009) Hydroxyapatite/MCM-41 and SBA-15 Nano-Composites: Preparation, Characterization and Applications, *Materials*, **2**, pp. 1508-1519

S. Brunauer, (1938) Adsorption of Gases in Multimolecular Layers, *J. Am. Chem. Soc.* 60, pp. 309–319.

J. C. P. Broekhoff, J. H. de Boer, (1968) Studies on pore systems in catalysts: XIII. Pore distributions from the desorption branch of a nitrogen sorption isotherm in the case of cylindrical pores B, Applications. *J. Catal*. 10, pp. 377–390.

D. Brunel, (2000) Adsorption of Gases in Multimolecular Layers, *New. J. Chem*, 24, pp. 807-813.

L. Jelinek, E. Kovhts, (1994) True surface areas from nitrogen adsorption experiments, Langmuir. 10, pp. 4225-4231.

L. Reinert, (2011) Characterization and boron adsorption of hydrothermally synthesised allophanes, *Appl. Clay. Sci* . 54 pp. 274-280.

L. Bois, (2003) Functionalized silica for heavy metal ions adsorption*, Colloid Surface A*. 221, pp. 221-230.

L. Liang, (2007) Defluoridation of drinking water by calcined MgAl–CO3 layered double hydroxides, *Desalination*, 208,pp. 125–133.